Addition of an Aminopeptidase N-Binding Sequence to Human Endostatin Improves Inhibition of Ovarian Carcinoma Growth

Yumi Yokoyama, Ph.D.[1]
Sundaram Ramakrishnan, Ph.D.[1–3]

[1] Department of Pharmacology, University of Minnesota, Minneapolis, Minnesota.

[2] Department of Obstetrics and Gynecology, University of Minnesota, Minneapolis, Minnesota.

[3] Comprehensive Cancer Center, University of Minnesota, Minneapolis, Minnesota.

Supported in part by a grant from the United States Army Medical Research and Materiel Command (DA/DAMD 17-99-1-9564), by the Minnesota Ovarian Cancer Alliance, and by the Sparboe Endowment/Women's Health Fund.

The authors thank Dr. Kathryn Burleson for editing the article.

Address for reprints: Sundaram Ramakrishnan, Ph.D., Department of Pharmacology, University of Minnesota, 6-120 Jackson Hall, 321 Church Street, S.E., Minneapolis, MN 55455; Fax: (612) 625 8408; E-mail: sunda001@umn.edu

Received November 22, 2004; revision received February 24, 2005; accepted March 3, 2005.

BACKGROUND. Blood vessels in tumors express higher level of aminopeptidase N (APN) compared with normal tissues. It has been reported that peptides that contain asparagine-glycine-arginine (NGR) sequence home to APN in tumor vasculature. Increased expression of APN in tumor vascular endothelium, therefore, offers an opportunity to target NGR peptide-linked therapeutic reagents to tumors.
METHODS. To determine whether an additional NGR sequence could improve endothelial homing and biologic activity, human endostatin was modified genetically to introduce an NGR motif (NGR-endostatin) and was expressed in yeast. In vitro biologic activity of NGR-endostatin was compared with the native protein in endothelial cell proliferation and migration. NGR-modified endostatin was used in tumor localization studies. Finally, the effects of endostatin and NGR-endostatin on tumor growth were determined in two model systems.
RESULTS. Human endostatin has an internal NGR sequence, which is not accessible to bind APN. However, the addition of an NGR-sequence at the amino terminus resulted in strong binding and inhibition of endothelial cell APN. NGR-endostatin showed increased binding to endothelial cells compared with the native protein. Increased binding of endostatin also coincided with improved antiangiogenic properties of endostatin. NGR modification improved tumor localization and, as a consequence, effectively inhibited ovarian carcinoma growth in athymic nude mice.
CONCLUSIONS. These studies demonstrated that human endostatin can be modified genetically to improve its ability to inhibit tumor growth. ***Cancer*** **2005;104: 321–31.** © *2005 American Cancer Society.*

KEYWORDS: endostatin, angiogenesis, asparagine—glycine—arginine (NGR), vascular targeting, aminopeptidase N, ovarian carcinoma.

Angiogenesis, the formation of new blood vessels from preexisting vasculature, is important for tumor growth and metastasis. CD13/aminopeptidase N (APN) is a Type II membrane-bound metalloproteinase (Mr 150,000), which cleaves amino terminal residues of biologically active peptides, such as enkephalins, angiotensins, neurokinins, and cytokines. APN is expressed in various epithelial cells, macrophages, and endothelial cells. CD13/APN originally was described as a lineage-specific marker for leukemias.[1] The appearance of CD13/APN coincides with commitment to myeloid lineage, and APN is expressed exclusively on normal and leukemic progeny of myeloid cells within the hematopoietic compartment. It also has been reported that APN is a receptor for coronavirus 229E, which is implicated in the etiology of severe acute respiratory syndrome.[2] Recent studies showed that APN is expressed at high levels in tumor vascu-

DOI 10.1002/cncr.21149
Published online 10 June 2005 in Wiley InterScience (www.interscience.wiley.com).

lature and plays an important role in angiogenesis. A unique peptide that contains NGR binds to APN in tumor vasculature.[3,4] APN is up-regulated in response to hypoxia and to angiogenic growth factors, such as basic fibroblast growth factor (bFGF) and vascular endothelial growth factor (VEGF), and it signals regulating capillary tube formation during angiogenesis.[5] Antibodies and functional inhibitors to APN blocked retinal neovascularization, chorioallantoic membrane angiogenesis, and tumor growth.[4] The NGR motif has been used for targeted delivery of tumor necrosis factor (TNF),[6] doxorubicin,[7] proapoptotic peptides,[8] and liposome.[9] A number of proteolytic fragments of endogenous proteins[10] and factors[11] are capable of inhibiting angiogenesis. The former group of inhibitors includes angiostatin,[10] encompassing kringle 1–4 of plasminogen; endostatin, a proteolytic fragment of a collagen Type XVIII[12]; a fragment of antithrombin[13]; and fragments of collagen IV, including tumstatin,[14] canstatin,[15] and arresten.[16] To determine whether an additional NGR sequence could improve endothelial cell homing and biologic activity, human endostatin was modified genetically to introduce an NGR motif and was expressed in yeast. Although endostatin has an internal NGR sequence (at position 126–128), this site is not accessible to bind and inhibit APN activity.[17] However, when an NGR sequence was added to the amino terminus of endostatin (NGR-endostatin), APN activity was inhibited significantly. NGR-endostatin showed improved inhibition of tumor growth.

MATERIALS AND METHODS

Cell Lines

Bovine adrenal gland capillary endothelial cells (BCE) were obtained from Clonetics Inc. (San Diego, CA). Human umbilical vein endothelial cells (HUVEC), passage 2, kindly were provided by Dr. Vercelotti (University of Minnesota). MA148, a human epithelial ovarian carcinoma cell line, was established locally at the University of Minnesota from a patient with Stage III epithelial ovarian serous adenocarcinoma.[18] The human primary melanoma cell line WM35 was provided by Dr. Iida and Dr. McCarthy (University of Minnesota). The human colon carcinoma cell line LS174T was obtained from the American Type Culture Collection (ATCC) (Rockville, MD). The mouse ovarian carcinoma cell line LM3 kindly was provided by Dr. Yokoro (Kyoto University, Japan). The human leukemic monocytic leukemia cell line U937 and the highly metastatic mouse melanoma cell line B16F10 were obtained from ATCC.

Antibodies

Antihuman APN monoclonal antibody (3D8) was obtained from NeoMarkers (Fremont, CA).

Cloning and Expression of Human Endostatin

Cloning and expression conditions of human endostatin have been published previously.[17] The yeast expression system of *Pichia pastoris* was purchased from Invitrogen (San Diego, CA). Restriction enzymes and Taq DNA polymerase were purchased from Boehringer Mannheim (Indianapolis, IN). To make NGR modification, the following sets of primers were used: up, TTCTCGAATTCAACGGGCGCCACAGCCACCGCGACTTCCAG; down, GGGGCGGCCGCCTACTTGGAGGCAGTCATGAAGCT.

Amplified fragments were purified, digested with EcoRl and Notl, and cloned into pPICZα-A vector. Plasmid DNA was then linearized at the Sacl site and used for homologous recombination into the yeast host strain X-33 (Invitrogen) by electroporation. Recombinant clones were selected on Zeocin-containing plates and were characterized for the expression of endostatins.

Purification of Recombinant Proteins

Pichia clones were cultured in baffled shaker flasks and induced by methanol as described previously. For large-scale preparations, a fermentation procedure was used. Endostatin and NGR-endostatin were purified by heparin affinity chromatography by following the published methods.[19] The heparin column was equilibrated with 10 mM Tris-HCl buffer, pH 7.6, and 0.5 mM phenylmethylsulfonyl fluoride (PMSF). Samples were applied to the column at a flow rate of 1.0 mL per minute with fast-performance liquid chromatography (Amersham Pharmacia Biotech, Piscataway, NJ). After thorough washing to remove unbound proteins, bound proteins were eluted with a continuous gradient of 0–1 M NaCl in 10 mM Tris-HCl, pH 7.6; and 0.5 mM PMSF. Both endostatin and NGR-endostatin were eluted at $\approx$ 0.5 M NaCl. Purified endostatins were analyzed on sodium dodecyl sulfate (SDS)-polyacrylamide gel electrophoresis gels (15% acrylamide gel) under reducing conditions.

Flow Cytometric Analysis

Expression levels of APN on a variety of cell lines were analyzed by flow cytometry. Cells were detached by 2 mM ethylenediamine tetraacetic acid (EDTA)/phosphate-buffered saline (PBS) and washed with Hank's balanced salt solution (HBSS). The cells were fixed with ice-cold 1% paraformaldehyde. After washing the cells with HBSS, a monoclonal antibody to APN (1:20 dilution) was added to the cells. Fluorescein isothio-

cyanate (FITC)-conjugated antimouse immunoglobulin G was used as the second antibody.

APN Activity

APN was extracted from cells, as described below (see Results), by lysis buffer (20 mM Tris-HCl, pH 7.6; 150 mM NaCl; 2 mM PMSF;, 10 μg/mL leupeptin; 0.5 mM *o*-vanadate; 20 mM N-ethyl-maleimide; and 2% Triton-X), and the enzymatic activity was determined using 0.225 mg (0.9 μmole) alanine p-nitroanilide as a substrate.[4] The cell lysate (10 μg protein) was incubated in a reaction buffer in the presence or absence of inhibitors at 37 °C for 2 hours. APN activity was measured by changes in absorbance at 405 nanometers (nm). Bestatin, a known APN inhibitor, was used as a positive control; and leupeptin, a serine protease inhibitor, was used as a negative control.

Cell Attachment Assay

One nanomolar per well of either endostatin or NGR-endostatin or 0.2% gelatin was used to coat 96-well enzyme-linked immunoadsorbent assay (ELISA) plates. The plates were incubated at 4 °C overnight and then blocked with 2% bovine serum albumin (BSA) in PBS at 37 °C for 2 hours. HUVEC or WM35 cells were harvested by 2 mM EDTA in PBS and prelabeled for 10 minutes at 37 °C with 5 μM 5-(and-6)-carboxy fluorescein diacetate, succinimidyl ester (5[6]-CFDA), a vital fluorescence dye (Molecular Probes, Eugene, OR). After washing with HBSS, fluorescence-labeled cells were resuspended in endothelial growth medium (HUVEC cells) or RPMI-1640 medium (WM35 cells). Cells were added to the wells at a density of 40,000 cells per well. After a 1-hour incubation at 37 °C, plates were washed twice with HBSS to remove unbound cells. Cells bound to the wells were detected by a fluorescence plate reader (Cyto Fluor II; PerSeptive Biosystems, Framingham, MA) (excitation; 485 nm, emission; 530 nm).

Endothelial Cell Proliferation Assay

Essentially, the method described by O'Reilly et al. was used.[12] Confluent BCE cells were trypsinized and resuspended in M199 (Invitrogen) medium with 5% fetal bovine serum (FBS). Cells were then seeded into gelatinized, 96-well culture plates at a density of 5000 cells per well. After 24 hours, endostatin or NGR-endostatin was added at a concentration of 2.5 μg/mL. Twenty minutes later, cultures were treated with 5 ng/mL of bFGF (Invitrogen). The viability of the control cells and the treated cells was determined by 5′-bromo-2′-deoxyuridine incorporation (Roche, Indianapolis, IN) according to the manufacturer's instructions.

Endothelial Cell Migration Assay

The migration of endothelial cells was determined by using Boyden chambers (Neuro Probe, Gaithersburg, MD). Polycarbonate filters (pore size, 12 μm) were coated with 0.2% gelatin for 1 hour at 37 °C. HUVEC cells were harvested in 2 mM EDTA in PBS and were prelabeled with 5 μM 5[6]-CFDA for 10 minutes at 37 °C. Cells were resuspended in 0.5% FBS and M199 medium and then preincubated with endostatin, NGR-endostatin, or SR-1 (an NGR-containing peptide) for 60 minutes at 37 °C. bFGF (25 μL of 25 ng/mL 0.5% FBS and M199 medium) was added to the lower chambers. HUVEC cells (200,000 cells/mL, control and treated) were added to the upper chambers. After 4 hours of incubation at 37 °C, endothelial cells that had migrated to the bottom side of the membrane were observed under a fluorescence microscope (Olympus, Melville, NY) using FITC filters (magnification, $\times$ 100). The captured images were quantified in the Adobe Photoshop (Adobe Systems, Inc., San Jose, CA) and MetaMorph (Molecular Devices Corporation, Downingtown, PA) programs. Two independent experiments were performed.

Tumor Localization

LS174T cells were injected subcutaneously in both sides of the flanks of female athymic nude mice (age 8 weeks). Tumor size reached $\approx$ 500 mm^3 in volume on Day 10. Tumor-bearing mice were randomized into two groups: a control group with seven mice and an experimental group with eight mice. Endostatin or NGR-endostatin was injected at a dose of 20 mg/kg subcutaneously. Nineteen hours after injection, tumor tissues (14 and 16 tumor samples from the respective groups) and representative normal tissues were removed surgically. This time point was chosen to minimize overwhelming serum levels from obscuring the tissue-bound endostatin. Tissues were snap frozen and homogenized in RIPA buffer containing proteinase inhibitors (PBS, 1% NP40, 0.5% sodium deoxycholate, 0.1% SDS, and 10 μg/mL PMSF), maintained at 4 °C for 45 minutes, and cleared by centrifugation. Human endostatin concentrations in the serum and in tissue lysates were determined by ELISA (Cytimmune, College Park, MD). The ELISA method showed similar sensitivity to both native endostatin and NGR-endostatin (data not shown). Statistical significance was determined with a Student *t* test.

Tumor Growth Inhibition Studies: Inhibition of Mouse Ovarian Carcinoma Growth in Athymic Nude Mice by Bolus Injection of NGR-Endostatin

Female athymic nude mice (age 4–6 weeks) were obtained from the National Cancer Institute and were

acclimatized to local conditions for 1 week. Logarithmically growing mouse ovarian carcinoma cells (LM3) were harvested by trypsinization and suspended in fresh medium at a density of 1×10^7 cells/mL. Then, 100 μL of the single-cell suspension were injected subcutaneously into the flanks of mice. When the tumors became visible (5 days after inoculation), mice were randomized into groups. The mice were treated with endostatin or NGR-endostatin subcutaneously at a dose of 20 mg/kg per day for 12 days. A control group of mice ($n = 5$ animals) was treated with sterile PBS under similar conditions. All injections were given subcutaneously $\approx$ 2 cm away from the growing tumor mass. Tumor growth was monitored by periodic caliper measurements. Tumor volume was calculated by the following formula: Tumor volume (mm^3) = ($a \times b^2$)/2, where a is the length in mm, and b is the width in mm ($a > b$). Statistical significance between control and treated groups was determined with a Student *t* test.

Inhibition of Human Ovarian Carcinoma in Athymic Nude Mice by NGR-Endostatin-Encapslated Alginate Beads

Endostatin-encapsulated alginate beads were prepared as described previously.[20] A control group of mice received vehicle-encapsulated alginate beads on a similar schedule. Alginic acid is a naturally occurring biopolymer that has been used as a matrix for entrapment and delivery of a variety of biologic agents. Logarithmically growing MA148 cells were harvested by trypsinization and suspended in serum-free medium at a density of 1×10^7 cells/mL. Then, 100 μL of the single-cell suspension were injected subcutaneously into the flanks of female athymic mice. When the tumors became visible (7 days after inoculation), mice were randomized into groups and were treated with endostatin-encapsulated alginate beads (5 animals per group). Because alginate microencapsultion results in slow and sustained release in vivo, endostatin preparations were given once a week (total, four injections) in this study. Statistical significance between control and treated groups was determined with a Student *t* test.

Determination of Vessel Density and Apoptosis

To determine the effect of antiangiogenic treatments on vessel density and apoptosis, residual tumors were resected surgically and snap frozen in liquid nitrogen. Cryostat sections (10 μm) of tumors were fixed in cold acetone, air dried, then treated with PBS containing 1% BSA to block nonspecific binding (background). Sections were then incubated with a 1:50 dilution of an anti-CD31 (mouse) monoclonal antibody conjugated to phycoerythrin (MEC 13.3; BD PharMingen, San Diego, CA). After a 1-hour incubation at room temperature, sections were washed thoroughly with PBS and then examined with an Olympus BX-60 fluorescence microscope. Images (7–10 fields per section) were captured by the Metamorph program for analysis. Detection of apoptosis was carried out by using an In Situ Cell Death Detection Kit (Boehringer Mannheim, Indianapolis, IN) following the manufacturer's protocol. Parts of the tumor samples were also fixed in 10% neutral buffered formalin and processed for histology.[20]

RESULTS

APN Expression and Activity in a Variety of Cells

The initial experiments were performed to determine expression levels of APN on ovarian carcinoma cell line, a melanoma cell line, and an endothelial cell line using flow-cytometric analysis (Fig. 1A). HUVEC cells expressed relatively larger amounts of APN compared with the ovarian and melanoma tumor cell lines. Flow-cytometric data showed that almost 100% of HUVEC cells were positive for APN expression.

Next, we examined functional levels of APN in lysates from a number of cell lines, including monocytoid U937 cells, which reportedly express APN.[21] Because APN is involved in the degradation of extracellular matrix (ECM) and invasion of metastatic tumor cells,[22] a highly metastatic mouse melanoma cell line, B16F10, was included in this study. APN activity from HUVEC cell lysates was much greater compared with APN activity in the carcinoma cell lines (Fig. 1B). bFGF treatment increased APN activity dramatically in HUVEC cells (Fig. 1C). After incubation with bFGF at a concentration of 20 ng/mL, the APN activity in HUVEC cells was 4.7 times greater than the activity in HUVEC cells without bFGF treatment. These data suggest that proangiogenic growth factors increase APN activity, which coincides with endothelial cell sprouting.[5]

APN Inhibited by NGR-Endostatin

We showed previously that the internal NGR sequence of endostatin is not accessible to APN; therefore, endostatin itself does not inhibit APN.[17] Endostatin was modified genetically to incorporate an NGR motif at the N-terminus, and the modified endostatin was investigated for its ability to inhibit APN. Endostatin containing an RGD sequence was used as a negative control.[20] Bestatin inhibited 35% of APN activity in HUVEC cell lysates. Endostatin and endostatin-RGD did not affect APN activity. However, NGR-endostatin inhibited APN activity by 17% at a concentration of 5 μM (Fig. 2A).

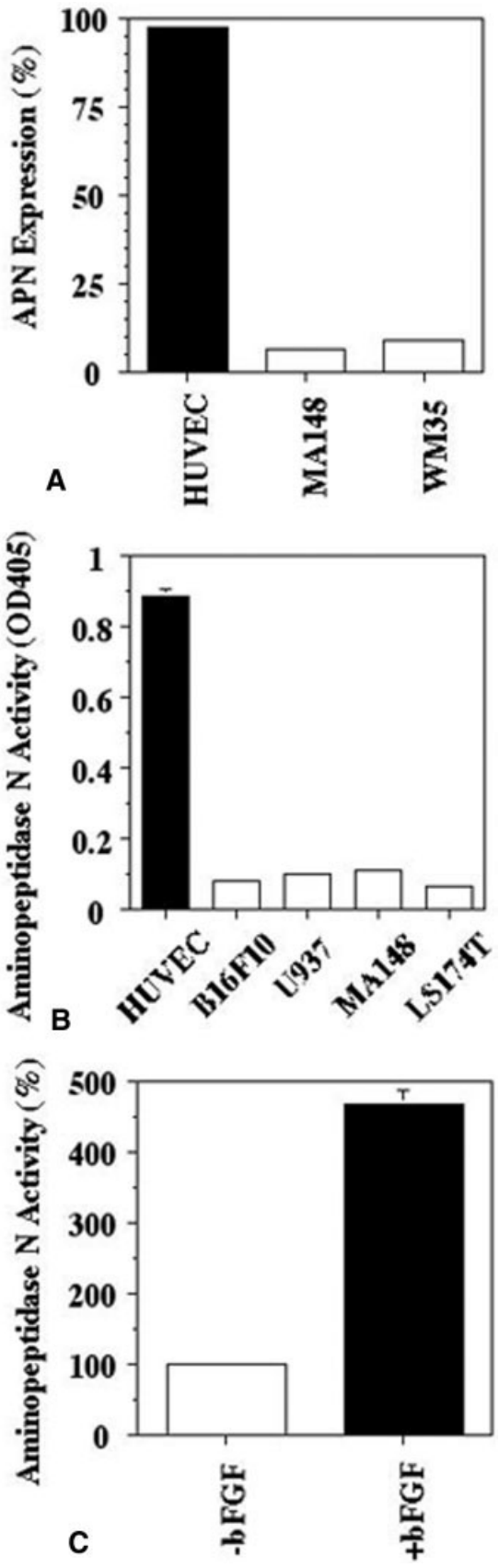

NGR Motif Increased Endothelial Cell Attachment to Endostatin

To determine whether the addition of an NGR motif to endostatin enhances binding to endothelial cells, cell-attachment assays were performed. For a positive control, 0.2% gelatin-coated wells were used. The extent of HUVEC cell attachment to gelatin-coated wells was used as 100% binding to calculate the relative efficiency of endostatin-mediated cell attachment. BSA-blocked wells were used as negative controls. Compared with gelatin, endostatin-coated wells showed $\approx$ 35% cell attachment (Fig. 2B). NGR modification of endostatin enhanced further the in vitro binding of endothelial cells. NGR-endostatin showed $\approx$ 60% cell attachment. This difference was significant. In contrast with HUVEC cells (97% APN-positive), most WM35 melanoma cells were APN-negative (8.8% positive) (Fig. 1). APN-negative WM35 cells did not show any increased attachment to NGR-endostatin. Both native endostatin and NGR-endostatin showed similar levels of basal attachment (Fig. 2B).

Increased Inhibition of Endothelial Cell Proliferation by NGR-Endostatin

Whether an NGR motif can affect the ability of endostatin to inhibit endothelial cell proliferation was evaluated (Fig. 2C). bFGF (5 ng/mL) was used as an inducer of endothelial cell proliferation. Endostatin treatment at 2.5 μg/mL inhibited bFGF-induced proliferation by 29%. Compared with native protein, NGR-endostatin treatment of HUVEC cells showed a marked improvement in inhibition of cell proliferation. NGR-endostatin showed 63% inhibition. This difference was statistically significant ($P = 0.032$).

Increased Inhibition of Endothelial Cell Migration by NGR-Endostatin

To evaluate whether an NGR motif can affect the ability of endostatin to inhibit endothelial cell migration, Boyden chamber-based migration assays were performed (Fig. 2D). bFGF was used as an inducer of endothelial cell migration. Endostatin treatment at 5 nM did not show inhibition of bFGF-induced migration. However NGR-modified endostatin showed complete inhibition of bFGF-induced endothelial cell

FIGURE 1. Expression and activity of aminopeptidase N (APN from a variety of cell lines: (A) Expression of APN from a variety of cell lines was analyzed by flow cytometry. (B) Enzymatic activity of APN was determined in cell lysates (10 μg protein). (C). Effect of basic fibroblast growth factor (bFGF) on APN activity in human umbilical vein endothelial cells (HUVEC).

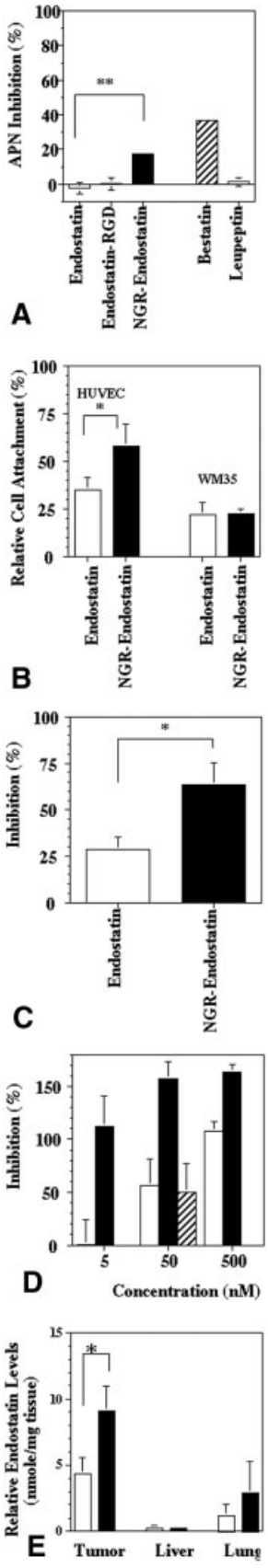

migration at 5 nM. At the higher concentrations, NGR-endostatin showed > 100% inhibition, indicating that even basal migration (in the absence of bFGF) was inhibited by NGR-endostatin. In a parallel study, NGR-containing synthetic peptide (SR-1) was admixed with native endostatin to determine whether the presence of NGR-peptide in the medium was sufficient to change the biologic activity of native endostatin. The data illustrated in Figure 2D show that admixing 50 nM endostatin along with the NGR synthetic peptide did not alter the basal level of endostatin-mediated inhibition of cell migration. The results from these studies suggest that an NGR moiety should be an integral part of endostatin to potentiate the biologic activity of endostatin.

Increased Tumor Localization of NGR-Endostatin

To assess whether the improved endothelial cell binding in vitro can translate into enhanced tumor homing in vivo, tumor localization studies were performed. Endostatin and NGR-endostatin were injected subcutaneously into human colon carcinoma-bearing athymic mice. Tumor, lung, liver, and serum samples were

FIGURE 2. Characterization of NGR sequence-modified endostatin (NGR-endostatin). (A) Aminopeptidase N (APN)-inhibitory activity. APN was extracted from human umbilical vein endothelial cell (HUVEC) cultures. Endostatin preparations, bestatin (positive control), and leupeptin (negative control) were used at a concentration of 5 μM. Endostatin-RGD: endostatin containing an RGD sequence. (B) Cell attachment assay. HUVEC or WM35 cells that were prelabeled with 5-(and-6)-carboxy fluorescein diacetate, succinimidyl ester, were added into triplicate wells coated with either endostatin or NGR-endostatin at a concentration of 1 nmole per well. Wells coated with 0.2% gelatin were used as maximum attachment (100%). The attached cells were quantified by a fluorescence plate reader. Values represent the mean of two independent experiments. (C) The effect of endostatin and NGR-endostatin on endothelial cell proliferation: Endostatin and NGR-endostatin were used at a concentration of 2.5 μg/mL. Basic fibroblast growth factor (5 ng/mL) was used to induce proliferation of endothelial cells. The proliferation was determined by 5′-bromo-2′-deoxyuridine uptake. (D) The effect of endostatin (open bar) and NGR-endostatin (solid bar) on HUVEC migration. NGR-containing peptide (SR-1) plus endostatin (hatched bar) did not enhance the basal level of inhibition seen with endostatin alone (open bar). (E) Tumor localization: Human colon carcinoma cells (LS174T) were injected subcutaneously into female athymic nude mice. When the tumors reached a size of $\approx$ 500 mm^3 (10 days after inoculation), endostatin (open bars) or NGR-endostatin (solid bars) was injected at a dose of 20 mg/kg subcutaneously. Tumor, liver, and lung tissues were resected and homogenized. Endostatin levels in the tissues and the sera were determined by enzyme-linked immunoadsorbent assay in the soluble fraction. Endostatin levels are expressed as a relative concentration to serum levels of endostatin. Error bars indicate the standard error. Statistical significance was determined with a Student t test. An asterisk indicates $P < 0.05$.

collected 19 hours after injection. Relative levels of endostatin in the tissues (compared with serum levels) are shown in Figure 2E. Native endostatin accumulated in the tumor tissues at a level of 4.3 nmole/mg tissue. Under similar conditions, NGR-endostatin showed 2-fold higher concentration in tumor tissue (9.1 nmole/mg tissue). Increased homing of NGR-endostatin was statistically significant.

Inhibition of Tumor Growth

To determine whether NGR-endostatin could improve the antitumor activity of endostatin, we used two tumor model systems. The first model systems used the mouse ovarian carcinoma cell line LM3. The second model used a human ovarian carcinoma cell line, MA148, in athymic nude mouse. In the first model system, bolus injections of endostatin were tested. NGR-endostatin and endostatin were administered subcutaneously at a dose of 20 mg/kg per day for the duration of the study. In this model system, the control tumors grew very rapidly and reached a size of $\approx$ 800 mm^3 by Day 17. Bolus injection of native endostatin inhibited tumor growth by $\approx$ 32.5% on Day 17 (Fig. 3A). Under similar conditions, NGR-endostatin treatment showed 50% inhibition.

Microencapsulation of Endostatin and NGR-Endostatin in Alginate Beads: Improved Antitumor Activity

NGR-endostatin inhibited tumor growth of MA148 cells more efficiently compared with native endostatin (Fig. 3B). Native endostatin-treated animals showed 58% inhibition in tumor growth. Tumor growth inhibition was improved significantly by treatment with NGR-endostatin. Approximately 73% inhibition was observed in the NGR-endostatin-treated group on Day 41 (statistically significant). Throughout the experiment, the NGR-endostatin-treated group showed reduced tumor volume compared with the native endostatin-treated group.

Inhibition of Tumor Angiogenesis

Figures 4A–C and 5A–C show that both endostatin treatment and NGR-endostatin treatment reduced blood vessel branch points (nodes), ends, and lengths significantly. The NGR motif enhanced the antiangiogenic effect of endostatin on the ends and lengths of blood vessels significantly. Terminal deoxyuridine triphosphate nick-end labeling and hematoxylin and eosin staining revealed that NGR-modified endostatin induced more apoptosis in tumor tissues, which is correlated with inadequate angiogenesis. A quantitative analysis of the apoptotic index is shown in Figure 5D. Endostatin-treated tumor tissues showed 22 apoptotic cells per field, whereas control tissues showed only 4.7 apoptotic cells per field. Greater numbers of apoptotic cells were seen in NGR-endostatin-treated mice. A mean of 47 apoptotic cells per field was seen in the NGR-endostatin-treated group.

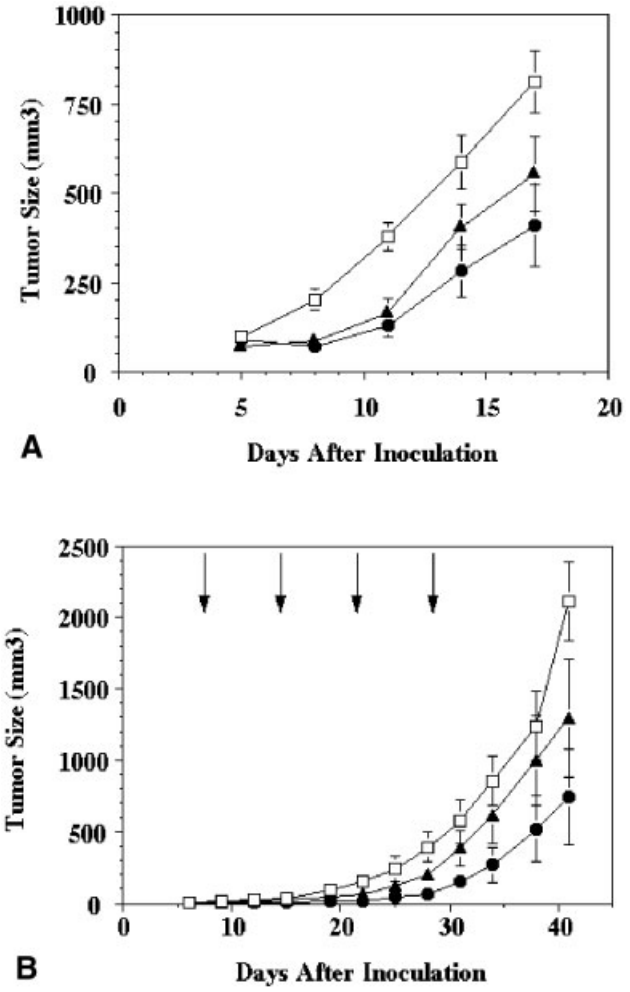

FIGURE 3. Improved inhibition of ovarian carcinoma by NGR sequence-modified endostatin (NGR-endostatin). (A) Bolus injection: The mouse ovarian carcinoma cell line, LM3, was injected subcutaneously into female athymic mice. After tumor establishment, mice were randomized and treated either with endostatin or with NGR-endostatin at a dose of 20 mg/kg per day. Treatment was continued for 12 days. Squares: phosphate-buffered saline control; triangles: endostatin; circles: NGR-endostatin. (B) Slow-release administration: Inhibition of human ovarian carcinoma (MA148) growth in athymic nude mice by NGR-endostatin encapsulated into alginate beads. Arrows represent treatment schedule. Squares: alginate bead control; triangles: endostatin; circles: NGR-endostatin. The mean tumor volume of control and treated groups are shown. Statistical significance was determined with a Student *t* test. Error bars indicate the standard error.

DICUSSION

Transmembrane proteases, such as membrane type matrix metalloproteinase, ADAM (a disintegrin and

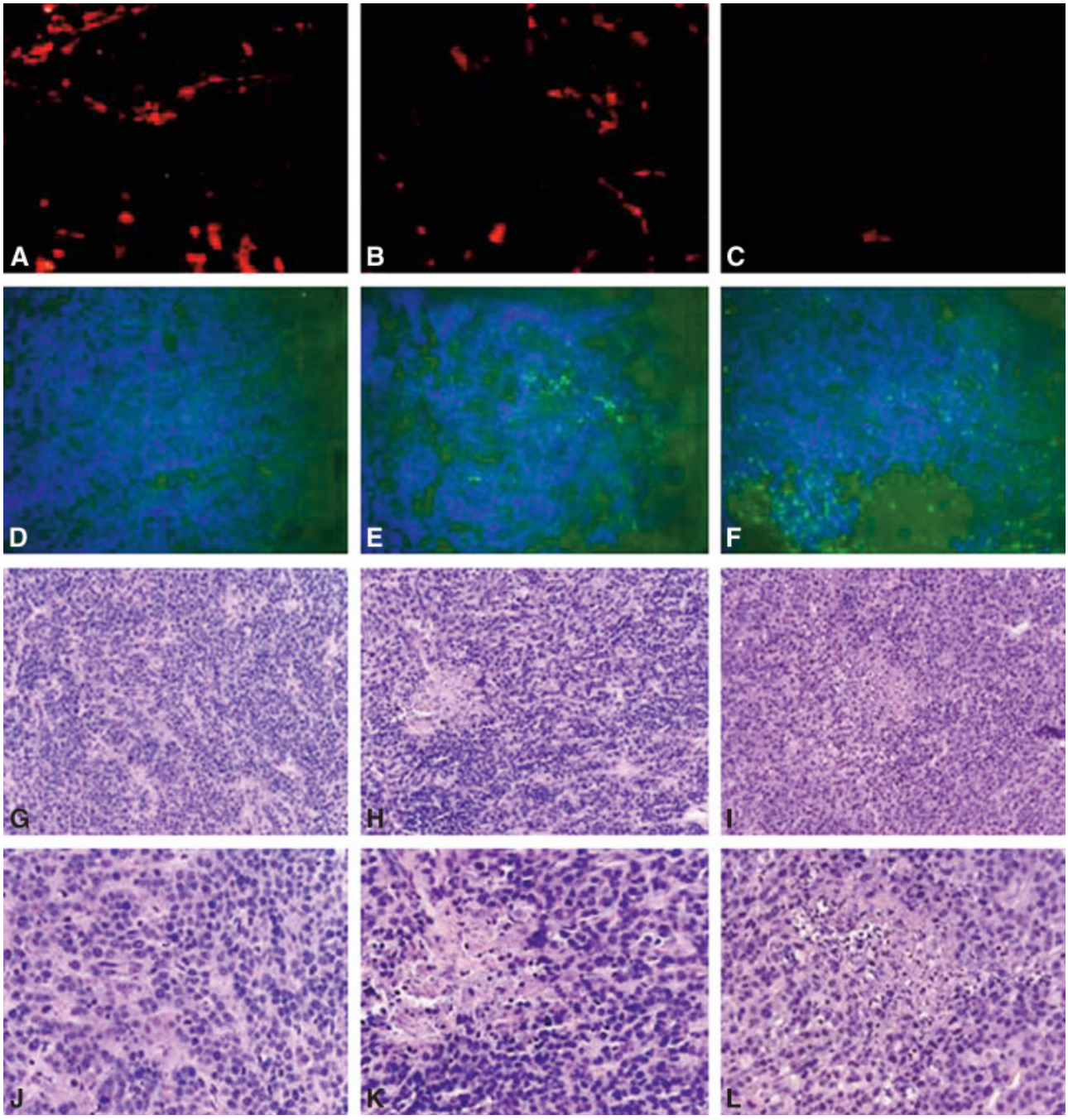

FIGURE 4. Apoptosis and histochemical analysis. Residual tumors from endostatin-treated groups and from NGR sequence-modified endostatin (NGR-endostatin)-treated groups were resected 1 day after the completion of treatment. A–C show vessel density, as determined by phycoerythrin-labeled, anti-CD31 antibody staining; D–F show terminal deoxyuridine triphosphate nick-end labeling assay (green) with 4,6-diamidino-2-phenylindole (blue); G–L show hematoxylin and eosin staining. A, D, G, and J are control sections; B, E, H, and K are endostatin-treated tumor sections; C, F, I, and L are NGR-endostatin-treated tumor sections. Original magnification ×100 (A–I); ×400 (J–L).

metalloprotease), and APN/CD13, are capable of degrading the ECM, leading to tumor cell invasion. Proteolysis of the ECM can also release sequestered angiogenic molecules. It has been reported that APN mediates the migration of human metastatic cell lines through matrigel.[23] APN also plays an important role in angiogenesis. APN expression is prognostic in patients with colon carcinoma.[24] Recent studies have shown that functional antagonists of APN (bestatin, actinonin, and anti-APN antibody) can inhibit tube

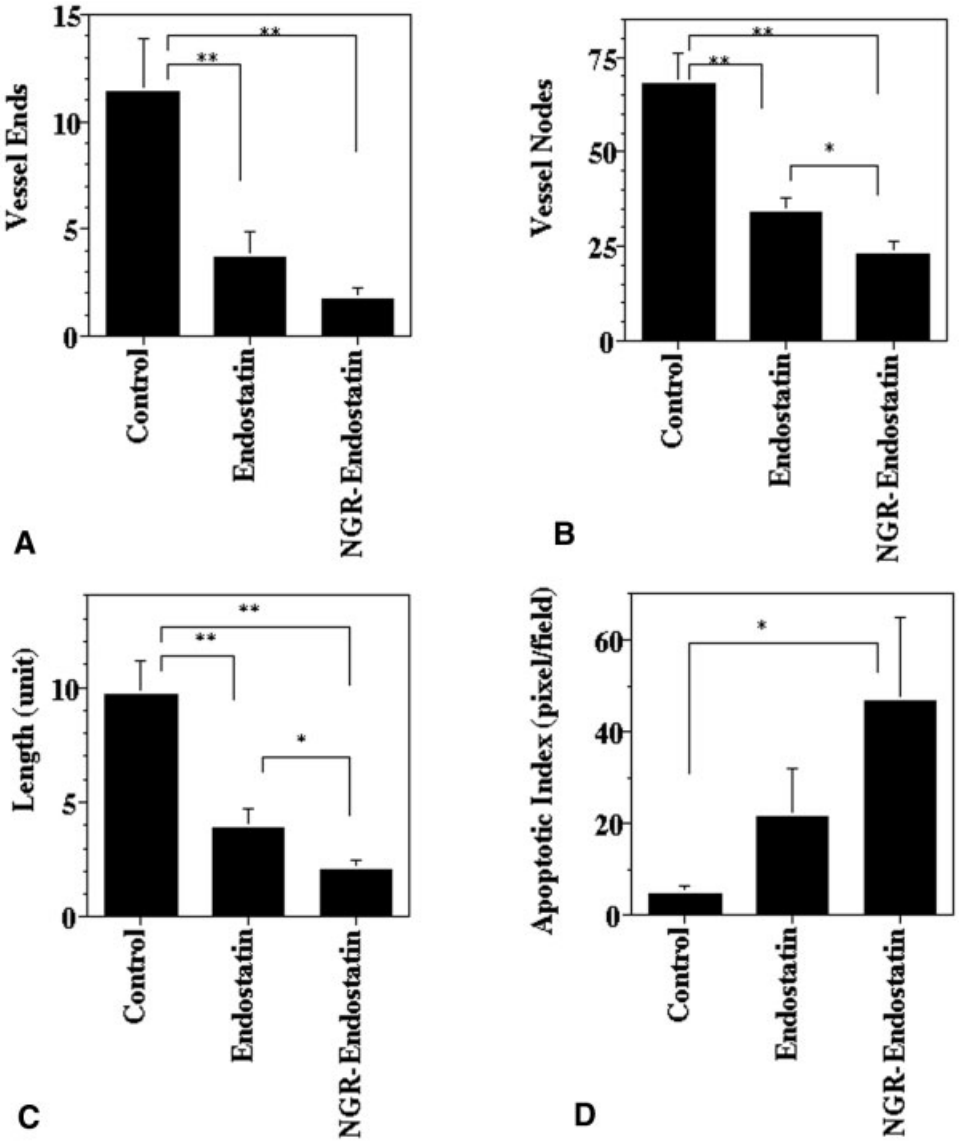

FIGURE 5. Quantification of antiangiogenic and apoptotic effect. Seven to 10 frames of tumor sections that were stained with antimouse CD31-phycoerythrin were captured per sample and then analyzed for microvessel density. (A) Blood vessel ends. (B) Branch points (vessel nodes). (C) Vessel length. (D) Quantification of apoptotic cells (pixel = cells) showed a marked increase in NGR sequence-modified endostatin (NGR-endostatin)-treated animals. Statistical significance was determined with a Student *t* test. Single asterisk: $P < 0.05$; double asterisks: $P < 0.01$. Error bars indicate the standard error.

formation and motility in endothelial cells without altering their proliferation.[4,24]

Recombinant endostain has been cloned and expressed in different expression systems. In some model systems, endostatin treatment either inhibited or regressed experimental tumors.[12] Other studies showed only moderate inhibition.[25] Bacterial expression systems often have resulted in insoluble proteins, necessitating a refolding protocol. It has been suggested that the slow release of endostatin from the insoluble suspension, coupled with proper refolding in vivo, is responsible for the potent inhibition of angiogenesis and tumor growth. Kranenburg et al. reported that a denatured, insoluble form of endostatin showed better bioactivity than a soluble form of endostatin.[26] Kruger et al. demonstrated the different efficacy between Calbiochem-endostatin and EntreMed-endostatin.[27] Genetic expression of human endostatin in bacteria and yeast seems to affect its biologic activity. Differences in potency and solubility characteristics, which reflect in part on protein folding, may explain the differences seen in endostatin efficacy in vivo. Understanding the basis for these discrepancies will aid in the successful clinical development of endostatin.

We showed previously that the antiangiogenic activity of endostatin can be improved by adding an integrin-targeting RGD sequence.[20] Because tumor blood vessels express higher levels of $\alpha_v\beta_3$ and $\alpha_v\beta_5$ integrins, an RGD motif increased the tumor localization and bioavailability of endostatin. In the current study, we evaluated whether an NGR motif also could

potentiate the activity of endostatin by virtue of binding to APN expressed on endothelial cells. We showed that an NGR motif increased endothelial cell attachment that was specific to APN expression. NGR-endostatin did not alter the basal binding of APN-negative WM35 melanoma cells. The data presented in the current study further validate the finding that the internal NGR sequence present in the native endostatin is not accessible to bind APN or to inhibit its enzymatic activity. The addition of an NGR motif to endostatin showed significant inhibition of APN activity in endothelial cell lysates. Furthermore, an NGR sequence at the amino terminus of endostatin enhanced the efficacy of endostatin to inhibit endothelial cell proliferation and migration. Curnis et al. showed that similar modification of TNF did not alter its affinity or biologic activity in vitro.[6] However, an NGR motif improved the efficacy of TNF in vivo. In the current study, we observed that the addition of an NGR sequence to endostatin increased its binding to endothelial cells and enhanced its biologic activity. No improvement in the biologic activity was seen when native endostatin was admixed with NGR peptides. These results suggest that enhanced inhibition of endothelial cells is dependent on an NGR motif in association with endostatin. In previous studies, doxorubicin conjugated with NGR peptides showed less toxicity to tumor cells in vitro (72 hours) compared with unconjugated doxorubicin.[7] However, NGR-conjugated doxorubicin showed better efficacy in vitro with a short exposure (20 minutes)[28] and inhibited tumor growth in vivo better compared with unconjugated doxorubicin.[7,28] Ellerby et al. showed that the biologic activity of a proapoptotic peptide $(KLAKLAK)_2$ was improved both in vitro and in vivo by an NGR motif.[8] Recently, Bhagwat et al. showed that inhibition of the angiogenic signal transduction pathway can be restored by the overexpression of APN.[29] Therefore, the blockage of APN activity by an NGR motif and the antiangiogenic effect of endostatin could act synergistically.

Because APN is expressed highly on tumor vasculature and the NGR-motif homes to APN, it is possible to target therapeutic molecules to the tumor vasculature. Pastorino et al. showed that liposome coupled with NGR had a longer circulating profile in blood and higher tumor localization compared with uncoupled liposome.[9] NGR-endostatin also localized to tumor tissues at a higher level compared with native endostatin. Increased accumulation of NGR-endostatin was correlated with greater antiangiogenic effects in vivo. Morphometric analysis revealed that NGR-endostatin treatment reduced vessel density in residual tumors. Decreased numbers of blood vessels coincided with increased apoptosis in tumor tissue. The results from these studies suggest that NGR modification of angiostatic molecules, such as endostatin, can be used to improve their therapeutic efficacy.

REFERENCES

1. Hogg N, Horton MJ. Myeloid antigens: new and previously defined clusters. New York: Oxford University Press, 1987.
2. Yeager CL, Ashmun RA, Williams RK, et al. Human aminopeptidase N is a receptor for human coronavirus 229E. *Nature.* 1992;357:420–422.
3. Arap W, Pasqualini R, Ruoslahti E. Cancer treatment by targeted drug delivery to tumor vasculature in a mouse model. *Science.* 1998;279:377–380.
4. Pasqualini R, Koivunen E, Kain R, et al. Aminopeptidase N is a receptor for tumor-homing peptides and a target for inhibiting angiogenesis. *Cancer Res.* 2000;60:722–727.
5. Bhagwat SV, Lahdenranta J, Giordano R, Arap W, Pasqualini R, Shapiro LH. CD13/APN is activated by angiogenic signals and is essential for capillary tube formation. *Blood.* 2001;97:652–659.
6. Curnis F, Sacchi A, Borgna L, Magni F, Gasparri A, Corti A. Enhancement of tumor necrosis factor alpha antitumor immunotherapeutic properties by targeted delivery to aminopeptidase N (CD13). *Nat Biotechnol.* 2000;18:1185–1190.
7. van Hensbergen Y, Broxterman HJ, Elderkamp YW, et al. A doxorubicin-CNGRC-peptide conjugate with prodrug properties. *Biochem Pharmacol.* 2002;63:897–908.
8. Ellerby HM, Arap W, Ellerby LM, et al. Anti-cancer activity of targeted pro-apoptotic peptides. *Nat Med.* 1999;5:1032–1038.
9. Pastorino F, Brignole C, Marimpietri D, et al. Vascular damage and anti-angiogenic effects of tumor vessel-targeted liposomal chemotherapy. *Cancer Res.* 2003;63:7400–7409.
10. Folkman J. Angiogenesis inhibitors generated by tumors. *Mol Med.* 1995;1:120–122.
11. Dawson DW, Volpert OV, Gillis P, et al. Pigment epithelium-derived factor: a potent inhibitor of angiogenesis. *Science.* 1999;285:245–248.
12. O'Reilly MS, Boehm T, Shing Y, et al. Endostatin: an endogenous inhibitor of angiogenesis and tumor growth. *Cell.* 1997;88:277–285.
13. O'Reilly MS, Pirie-Shepherd S, Lane WS, Folkman J. Antiangiogenic activity of the cleaved conformation of the serpin antithrombin. *Science.* 1999;285:1926–1928.
14. Maeshima Y, Sudhakar A, Lively JC, et al. Tumstatin, an endothelial cell-specific inhibitor of protein synthesis. *Science.* 2002;295:140–143.
15. Kamphaus GD, Colorado PC, Panka DJ, et al. Canstatin, a novel matrix-derived inhibitor of angiogenesis and tumor growth. *J Biol Chem.* 2000;275:1209–1215.
16. Colorado PC, Torre A, Kamphaus G, et al. Anti-angiogenic cues from vascular basement membrane collagen. *Cancer Res.* 2000;60:2520–2526.
17. Yokoyama Y, Ramakrishnan S. Improved biological activity of a mutant endostatin containing a single amino-acid substitution. *Br J Cancer.* 2004;90:1627–1635.
18. Ramakrishnan S, Olson TA, Bautch VL, Mohanraj D. Vascular endothelial growth factor-toxin conjugate specifically inhibits KDR/flk-1-positive endothelial cell proliferation in vitro and angiogenesis in vivo. *Cancer Res.* 1996;56:1324–1330.

19. Yokoyama Y, Dhanabal M, Griffioen AW, Sukhatme VP, Ramakrishnan S. Synergy between angiostatin and endostatin: inhibition of ovarian cancer growth. *Cancer Res.* 2000;60: 2190–2196.
20. Yokoyama Y, Ramakrishnan S. Addition of integrin binding sequence to a mutant human endostatin improves inhibition of tumor growth. *Int J Cancer.* 2004;111:839–848.
21. Wex T, Lendeckel U, Wex H, Frank K, Ansorge S. Quantification of aminopeptidase N mRNA in T cells by competitive PCR. *FEBS Lett.* 1995;374:341–344.
22. Hidaka S, Funakoshi T, Shimada H, Tsuruoka M, Kojima S. Comparative effects of diethyldithiocarbamate and N-benzyl-D-glucamine dithiocarbamate on cis-diamminedichloroplatinum-induced toxicity in kidney and gastrointestinal tract in rats. *J Appl Toxicol.* 1995;15:267–273.
23. Riemann D, Kehlen A, Langner J. CD13—not just a marker in leukemia typing. *Immunol Today.* 1999;20:83–88.
24. Hashida H, Takabayashi A, Kanai M, et al. Aminopeptidase N is involved in cell motility and angiogenesis: its clinical significance in human colon cancer. *Gastroenterology.* 2002; 122:376–386.
25. Dhanabal M, Ramchandran R, Waterman MJ, et al. Endostatin induces endothelial cell apoptosis. *J Biol Chem.* 1999;274: 11721–11726.
26. Kranenburg O, Kroon-Batenburg LM, Reijerkerk A, Wu YP, Voest EE, Gebbink MF. Recombinant endostatin forms amyloid fibrils that bind and are cytotoxic to murine neuroblastoma cells in vitro. *FEBS Lett.* 2003;539:149–155.
27. Kruger EA, Duray PH, Tsokos MG, et al. Endostatin inhibits microvessel formation in the ex vivo rat aortic ring angiogenesis assay. *Biochem Biophys Res Commun.* 2000;268:183–191.
28. Arap W, Pasqualini R, Ruoslahti E. Cancer treatment by targeted drug delivery to tumor vasculature in a mouse model. *Science.* 1998;279:377–380.
29. Bhagwat SV, Petrovic N, Okamoto Y, Shapiro LH. The angiogenic regulator CD13/APN is a transcriptional target of Ras signaling pathways in endothelial morphogenesis. *Blood.* 2003;101:1818–1826.